JCTC Journal of Chemical Theory and Computation

Solvent Effects on Donor−Acceptor Couplings in Peptides. A Combined QM and MD Study

Frank Wallrapp,[†] Alexander Voityuk,*[,‡] and Victor Guallar*[,†]

Catalan Institució Catalana de Recerca i Estudis Avançats, 08010 barcelona, and Life Science Program, Barcelona Supercomputing Center, Nexus II Building, 08028 Barcelona, Spain, and Institució Catalana de Recerca i Estudis Avançats, 08010 Barcelona, and Institut de Química Computational, Universitat de Girona, 17071 Girona, Spain; Catalan Institution for Research and Advanced Studies, Institute of Computational Chemistry, Department of Chemistry, University of Girona, 17071 Girona, Spain

Received July 20, 2009

Abstract: We present a combined Quantum Chemical/Molecular Dynamics study on electronic coupling between tryptophan-based donor and acceptor in oligopeptides of variable length. Molecular dynamics was performed on Trp-(Pro)n-Trp ($n = 1$ to 6) molecules in gas phase and aqueous solvent and the electronic coupling matrix element was computed for thermal hole transfer applying semiempirical INDO/S together with the generalized Mulliken-Hush approach. For comparison, we also computed coupling values of 40 000 snapshots applying ab initio Hartree−Fock, showing good agreement with the INDO/S results. We demonstrate that the coupling values strongly fluctuate throughout the molecular dynamic trajectory and the mechanism of electron transfer is affected by the presence of solvent through restriction of the conformational space. Gas-phase calculations show gated electron transfer dominated by direct through-space coupling due to strong conformational changes bringing donor and acceptor in close vicinity. Solvent calculations establish a nongated mechanism dominated by bridge-mediated coupling. In agreement with experimental data, our results point to a donor−acceptor distance of ∼20 Å as a possible point for transition from superexchange to hopping electron transfer mechanism.

I. Introduction

Protein-mediated electron transfer (ET) between separated local donor and acceptor sites plays a central role in biochemistry.[1−5] For example, long-range electron transfer over a distance of 10 to 30 Å is a process of major importance in photosynthesis and respiration. In general, electron transfer can be considered as a transition between electronic states. Its rate is determined both by the coupling between those electronic states and by the reorganization energy needed by the system to adapt to its new state. Although the motion of the electron is in fact instantaneously on the time scale of nuclear motion, the rate of electron transfer is generally slow when compared to that. Rate constants can vary over many orders of magnitude due to the roughly exponential dependence of the electronic-state overlap on the donor−acceptor distance.[6] Variations of this distance dependence has been the subject of a dynamic discussion between experimentalists[7−9] and theoreticians[10,11] in the last years and is still ongoing. Many of these studies have focused on test systems of single-chained short oligopeptides to get an easier understanding of the underlying ET mechanism. Despite bridge-mediated superexchange between donor and acceptor, electron transfer can also occur through a process of incoherent hopping between localized electronic states on the bridge.[12] The respective contributions

* Corresponding authors: Victor Guallar: victor.guallar@bsc.es; Alexander Voityuk: alexander.voityuk@icrea.es.

[†] Barcelona Supercomputing Center.

[‡] University of Girona.

10.1021/ct900377j CCC: $40.75
Published on Web 10/29/2009

of the two mechanisms are dependent on the energy difference between the donor- and bridge-localized electronic states. The total rate constant of the system is then the composite of both bridge-mediated superexchange and sequential hopping mechanism. Experimental work on oligoproline between Ruthenium based donors and acceptors has shown that electron transfer mechanism can also change from a predominantly electron superexchange to a predominantly electron hopping mechanism when the peptide spacer distance exceeds about 20 Å.[13] Furthermore, recent studies on protein electron transfer emphasize the importance of tryptophans within these multistep electron transfers.[14,15]

Next to the distance, dynamical flexibility of the protein and solvent has also a strong impact on the electronic coupling between donor and acceptor. Recently there have been several studies describing how conformational dynamics of proteins strongly influence the donor−acceptor coupling,[6,16−24] showing that these observed fluctuations can be large and sometimes within only the femtosecond time scale. Also, a recent study on through-bond electron transfer in Ru-modified azurin indicates the central role of valence angle fluctuations in coupling dephasing.[25] Furthermore, there exist recent studies on U-shaped electron transfer systems where a highly curved bridge imparts a vacant cleft along the line-of-sight between the electron donor and acceptor.[26−28] Semiempirical calculations show that electronic coupling between donor and acceptor within these model systems results mainly from direct coupling or coupling through bridging solvent molecules. This feature differs strongly from craned model systems in which the coupling is mainly due to through-bond contributions resulting in a linear decrease of direct coupling with larger donor−acceptor distance.[29−31] To capture the dynamical behavior of the electronic coupling, it is necessary to calculate the average over many snapshots of a long molecular dynamics trajectory to cover full conformational space of flexible model systems.[16]

The electronic coupling for the hole transfer process can be calculated using the one-electron or Koopmans' theorem approximation.[32,33] Within this scheme, the desired properties of the adiabatic states for a radical cation can be approximated using one-electron energies and occupied molecular orbitals of the corresponding neutral (close-shell) system.[34] Computing the electronic coupling for large systems is a challenge due to the amount of atoms involved in the electron transfer. Avoiding the computational effort to calculate donor−acceptor coupling values from ab initio calculations,[35] there exist several semiempirical approaches, which allow analyzing the coupling of large proteins over many snapshots. Among them are Extended-Hückel related methods[21,36,37] and the neglect of differential overlap (INDO/S).[38] Unlike the standard semiempirical schemes based on the NDDO approximation (MNDO, AM1 and PM3), the INDO/S method provides surprisingly good results for electronic couplings[39] and thus is widely accepted as a feasible approximation for ET calculations, being subject of much comparison against ab initio calculations.[6,40,41]

The aim of this article is to study the mechanism of thermal hole transfer in oligopeptides in gas phase as well as aqueous solution. Therefore, we calculate coupling values from

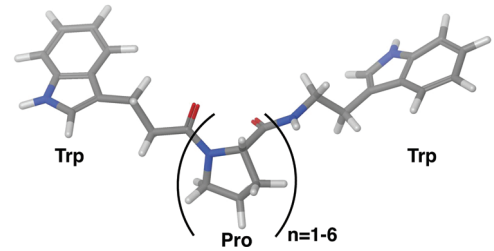

Figure 1. Trp-(Pro)n-Trp in gas phase.

electronic properties derived from semiempirical INDO/S calculations as well as more sophisticated Hartree−Fock (HF) calculations to compare both levels of theory against each other. The results show that the mechanism is highly affected by the presence of solvent by means of restricting the conformational space within the dynamics. On the basis of recent studies on protein electron transfer indicating the importance of tryptophans,[14,15] we used a set of oligoproline peptides of variable length linking tryptophan based electron donors (D) and acceptors (A) as our test system.

II. Methods

Modeling Oligopeptide Structure and Dynamics. Oligopeptide Trp-(Pro)n-Trp with n from 1 to 6 was assembled using Schrödinger's Maestro[42] build utility, having the amino group of the donor Trp and the acetyl group of the acceptor Trp replaced by hydrogen atoms. For each peptide, we prepared two different setups for the molecular dynamics (MD): in gas phase and in aqueous solvent. Figure 1 shows Trp-(Pro)n-Trp in gas phase as an example. For all of the systems, we performed a 10 ns NVT trajectory at 298.15 K, following a truncated Newton minimization and a short equilibration (10 ps for vacuum and 100 ps for solvent). For the $n = 4$ case, we performed an additional 30 ns trajectory in solvent to compare its mean donor−acceptor distance and mean coupling value against the 10 ns trajectory. Snapshots for the electronic coupling calculation were saved every picosecond based on a donor−acceptor autocorrelation analysis of the highly mobile system Trp-Pro2-Trp in gas phase. Further explanation to this as well as the distance autocorrelation plot is given in the Supporting Information. Vacuum minimization, equilibration, and MD simulations were performed with *Impact*[43] using a nonbonded cutoff value of 12 Å. Solvent simulation applied the SPC water model[44] in a cubic box of 10 Å buffer region, periodic boundary condition, and the Ewald summations. Solvent MD was performed with *Desmond*.[45] The applied force field throughout all the MD simulations was OPLS-2005.[46] From the production run, we extracted 10 000 snapshots, which in the solvent cases include only a layer of 4 Å of waters around the backbone of the oligopeptide to keep computational time of the electronic properties calculations as low as possible.

Electronic Couplings. In biochemistry, many electron transfer reaction haves only weak electronic coupling between donors and acceptors. In this case, the ET rate can be described by Marcus theory by the following high-temperature nonadiabatic expression:[1]

$$k_{ET} = \frac{2\pi}{\hbar} V_{DA}^2 \frac{1}{\sqrt{4\pi\lambda k_B T}} \exp\left(\frac{-(\lambda + \Delta G^\circ)^2}{4\lambda k_B T}\right) \quad (1)$$

Here, V_{DA} is the electronic coupling between the diabatic donor and acceptor states, $\hbar$ is Planck's constant, k_B is Boltzmann's constant, λ is the reorganization energy, T is the temperature, and ΔG° is the overall Gibbs free energy change of the electron transfer reaction. The coupling can be derived by applying the generalized Mulliken-Hush method (GMH)[29,30] using electronic properties of the adiabatic states of the system. How to apply the GMH scheme within the one-electron picture of hole transfer is considered in detail elsewhere.[47] For simple systems like the one to which we have applied a two-state model is a good approximation, whereas for more sophisticated systems the multistate model with bridge states has to be considered. Applying the two-state model, the bridge-mediated electronic coupling can be calculated through the following formula:

$$V_{DA} = \frac{\Delta E_{12} |\mu_{12}|}{|\mu_D - \mu_A|} \quad (2)$$

where $\Delta E_{12} = E_1 - E_2$ is the vertical excitation energy with E_1 and E_2 being the energies of the two relevant adiabatic states. μ_{12} is the transition dipole moment and $|\mu_D - \mu_A|$ is the difference of the diabatic dipole moments. Here, we can estimate $|\mu_D - \mu_A|$ as ed_{DA} or as $((\mu_1 - \mu_2)^2 + 4\,\mu_{12}^2)^{1/2}$.[29,30] Here, it is important to use only the projection of the transition and dipole moments onto the axis between the donor and acceptor rather than the length of the vectors. Furthermore, it is assumed that the two-state system is only weakly coupled, meaning $V_{DA} < k_B T$. Koopmans' theorem states that the energies of occupied molecular orbitals for a closed-shell system approximate the (negative) vertical ionization potentials ($-IP$).[32,33,48] On the basis of this theorem, the adiabatic splitting, E_{12}, is computed from the energy difference of the highest occupied molecular orbital (HOMO) and the next-highest occupied molecular orbital (HOMO-1) of the neutral system approximating the two quasi-degenerate electronic eigenstates of the ET system. We are aware of the approximate description of the hole transfer process in the systems considered. In particular, MD treatment of radical cation states of oligopeptides (explicit presence of a hole) can lead to structures that somewhat deviate from the generated structures within this study. However, we believe that averaging of the couplings over many thousand conformations make our estimates quite robust.

Quantum Mechanical Calculations. We carried out two different levels of theory to derive the electron transfer parameters, the semiempirical method INDO/S[38] and ab initio HF. The INDO/S calculations on the neutral oligopeptides are carried out on all 10 000 snapshots of every trajectory of Trp-(Pro)n-Trp with n from 1 to 6. We further distinguish systems simulated in gas phase, systems simulated in explicit solvent but solvent molecules omitted from electronic property calculations (latterly denoted as *solvated-conformation-only*), and finally systems simulated in water keeping a layer of 4 Å of waters around backbone of oligopeptide (latterly denoted as *solvated*). Within the calculations, an average of 2.75% of the models had to be omitted due to the rare case of HOMO and HOMO-1 orbitals localizing into the same site and thus making the coupling meaningless in the sense of electron transfer between the two tryptophans. All ab initio Hartree−Fock calculations were performed with *Jaguar*.[49] We carried out single point energy calculations on all snapshots on solvated Trp-(Pro)3-Trp and Trp(Pro)6-Trp with and without the water molecules included as point charges in the quantum chemical calculations. We applied the 6-31G* basis set on all atoms resulting in 774 basis functions for Trp-(Pro)3-Trp and 1131 basis functions for Trp-(Pro)6-Trp.

Statistical Analysis. We performed all data analyses with the open source software package R.[50] For one of these, we applied the multivariate regression statistical method Partial Least Squares regression (PLS-R),[51] which is used to find the fundamental relations between two matrices X and Y. The method works by finding the multidimensional direction in the X space that explains the maximum multidimensional variance direction in the Y space, describing both X and Y by a few latent variables also known as principal components (PC). PLS-R models are usually built by extracting successive PCs, each one increasing the total percentage of Y variance explained given by cumulative Q2, until the predictive ability of the model is optimized. PLS-R is particularly suited when there is multicollinearity among the X values, where, by contrast, standard regression methods will fail. A further advantage is the ability to extract information about both the objects and the variables. The objects can be represented graphically according to the PC values, obtaining highly informative score plots in which similar objects appear as points closely situated in the space. In addition, the original variables can also be represented according to their overall contribution to the model by coefficient plots. These plots provide information about which variables exhibit a relevant association with the dependent variable, the direction of it, and if this association is statistically significant.

III. Results and Discussion

Molecular Dynamics. The classical molecular dynamics trajectories of the oligopeptide reveal a substantial mobility of the peptide chains. Figure 2 shows the donor−acceptor distance d_{DA}, measured between the middle of bond CD2-CE2 of the respective tryptophans, of all systems in gas phase as well as in solvent. We checked the reliability of the average values of the 10 ns trajectories by calculating d_{DA} from a 30 ns trajectory for Trp-(Pro)4-Trp in solvent. The resulting average for 30 ns (Pro4*) has no significant difference to 10 ns, indicating that the applied 10 ns trajectories are representative for the behavior of the systems.

There are several insights derived from this plot. First, mean d_{DA} of every oligopeptide system is smaller in gas phase than in solvent and second the variance of the distance is higher in gas phase than in solvent, indicated by the box size in Figure 2. Also, the minimum separation of the two tryptophans in gas phase is a constant of about 5 Å. This shows that the oligopeptides in gas phase undergo strong

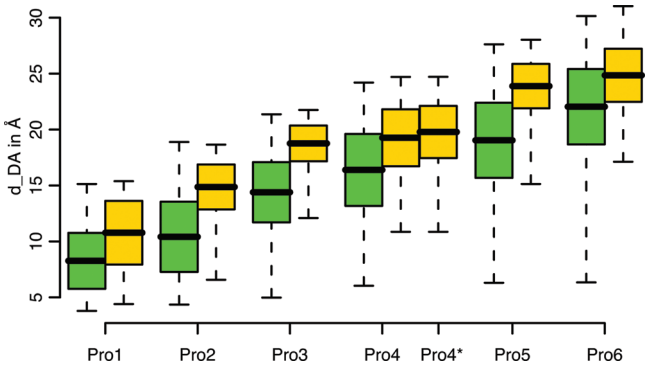

Figure 2. Donor−acceptor distance d_{DA} in Å for 10 ns trajectory of oligopeptides in gas phase (green) and solvent (yellow). d_{DA} of Pro4 in solvent for 30 ns trajectory is indicated with an asterisk. Black bar shows mean value, box captures values between $-\sigma$ and $+\sigma$ and dashed lines indicate minimum and maximum values of respective distribution.

conformational changes and even collapse, bringing the two tryptophans in very close vicinity to each other during the MD. The oligopeptides simulated in solvent also undergo conformational changes but not as extreme and quick as those in gas phase, also they stay more craned and never collapse.

Electronic Couplings. We calculated the bridge-mediated electronic coupling between the donor and acceptor for every single snapshot as denoted above in eq 2 with parameters derived from INDO/S calculations on the three different trajectory types mentioned above: gas phase, solvated-conformation-only, and solvated. For direct comparison we also calculated coupling values in HF level of theory for solvated Trp-(Pro)n-Trp with $n = 3$ and 6 with and without the waters included as point charges. All rms V_{DA} values are shown in Table 1. The data shows that there is no significant difference between INDO/S and HF indicating the high accuracy of the semiempirical INDO/S method in the calculation of electronic couplings. We also included coupling values calculated for the 30 ns solvated-conformation-only trajectory on Trp-(Pro)4-Trp, having a mean coupling value of 2.42×10^{-5} eV (GMH). This value differs only marginally from the mean coupling value derived from the 10 ns trajectory, being 3.02×10^{-5} eV, indicating that a sample size of 10 000 snapshots is sufficient for electronic coupling calculations of the applied oligoproline systems. Further cross checking also revealed excellent agreement between V_{DA} computed by GMH and V_{DA} computed with charge fragment difference method (FCM).[47] Figure 3 shows the rms V_{DA} (GMH) plotted against mean d_{DA} of the respective trajectories. It can be seen that there is an increasing gap between the coupling values calculated for the oligopeptides simulated in gas phase and those simulated in solvent. Figure 3 points out that these differences are not only based upon longer mean d_{DA} within the solvated trajectories but also rely on further conformational effects of the solvent, which becomes larger with increasing n. There is no significant difference between rms V_{DA} computed from solvated oligopeptides including or excluding the waters within INDO/S calculations, which points out that the electronic properties of the water molecules do not contribute to the coupling of the two tryptophans. Therefore, we will only focus on oligopeptides simulated in gas phase as well as in solvent, omitting the waters within the INDO/S calculations (solvated-conformation-only) in the following analyses.

Gated/Nongated Mechanism. It is known from the literature that electronic coupling can strongly depend on the conformation of the system.[52] In the so-called conformationally gated electron transfer, the charge is not gradually transferred from the donor to the acceptor instead there is a sudden jump enhanced by favorable conformations with high electronic coupling between donor and acceptor. Tracking the rate of conformational gating of the electron transfer in the different oligoproline systems, we plotted the distributions of the data by histograms of V^2_{DA}. The data is sorted and clustered by number of standard deviations above the total mean value of V^2_{DA}, called z-score. For each cluster, we then plotted the fraction of mean V^2_{DA} given by its data points against its z-score. Values of coupling being higher than 100 times the standard deviation are accumulated into the last cluster. The results for gas-phase trajectories are given in Figure 4. Here, the plots show a trend of increasing conformational gating with increasing number of prolines. As already discussed above, with growing number of bridge prolines, the mean distance between donor and acceptor d_{DA} becomes larger as well (shown in Figure 2). Thus, the coupling values associated with the conformations around the mean distance value decrease significantly. The dashed lines in Figure 2 also indicate the large mobility for the gas-phase systems. For any number of bridge prolines, we find few snapshots with very short d_{DA}, associated with high coupling values. The results indicate that the contribution of these few snapshots to the mean value increases with the number of prolines, establishing a gated mechanism for $n > 2$. A closer inspection at this $n = 3$ transition point indicates a critical mean distance around ∼15 Å. If a system with this mean value is capable of visiting conformations with d_{DA} ∼7 Å, then the overall ET mechanism might be gated.

The results for the solvated trajectories are given in Figure 5. As expected, the overall results for the electron transfer in presence of water shows a nongated mechanism; only Pro2 lies on the border of conformational gating. This result can be rationalized in terms of the mean and extreme donor−acceptor distance observations deduced in the gas-phase studies. As seen in Figure 2, in the presence of water the extreme (lower) donor−acceptor distances are much higher than in gas phase for each trajectory. Only in the case of Pro2 we observe mean distances ∼15 Å together with low extreme d_{DA} values close to 7 Å.

Direct/Bridge-Mediated Coupling. We also calculated the direct coupling between donor and acceptor, skipping the bridging prolines within the INDO/S calculations. From estimating $|\mu_D - \mu_A|$ through ed_{DA} in eq 2, we know that direct coupling is inversely proportional to d_{DA}. Hence, we expect decreasing direct coupling values for oligopeptide systems with increasing n due to increasing mean d_{DA}. Figure 6 shows both bridge-mediated coupling (solid lines) as well as direct coupling (dashed lines) from gas phase (black) and solvated-conformation-only (red) plotted against respective d_{DA}. In gas phase, direct couplings are essentially the same

Table 1. Rms V_{DA} Values in eV Calculated for Oligopeptide Systems with the INDO/S and HF Method

		gas phase		solvated-conf.-only		solvated	
prolines	method	GMH	FCM	GHM	FCM	GHM	FCM
1	INDO/S	2.18×10^{-2}	2.17×10^{-2}	1.95×10^{-2}	1.94×10^{-2}	1.95×10^{-2}	1.94×10^{-2}
2	INDO/S	9.74×10^{-3}	9.68×10^{-3}	1.47×10^{-3}	1.46×10^{-3}	1.51×10^{-3}	1.46×10^{-3}
3	INDO/S	1.95×10^{-3}	1.94×10^{-3}	1.19×10^{-4}	1.19×10^{-4}	1.04×10^{-4}	1.19×10^{-4}
	HF			1.61×10^{-4}	1.61×10^{-4}	1.49×10^{-4}	1.51×10^{-4}
4	INDO/S	1.16×10^{-3}	1.16×10^{-3}	3.02×10^{-5}	3.03×10^{-5}	2.78×10^{-5}	2.79×10^{-5}
4 (30 ns)	INDO/S			2.42×10^{-5}	2.44×10^{-5}		
5	INDO/S	3.79×10^{-4}	3.79×10^{-4}	4.36×10^{-8}	4.37×10^{-8}	4.39×10^{-8}	
6	INDO/S	1.25×10^{-4}	1.25×10^{-4}	7.36×10^{-8}	7.37×10^{-8}	6.58×10^{-8}	
	HF			2.48×10^{-7}	2.32×10^{-7}	7.25×10^{-8}	

as bridge-mediated couplings, which can be explained by conformational gating. As described above, in gas phase only conformations of very short d_{DA} contribute to the mean coupling V_{DA}. Here, direct couplings between donor and acceptor are also high, consequently summing up to equal mean V_{DA}. Direct coupling values calculated on solvent trajectories show expected behavior, being much lower than bridge-mediated coupling values. Here, in contrast to the gas phase, mean d_{DA} and also lower extreme d_{DA} are increasing with n and thus direct couplings drop significantly because of their inverse proportionality to distance. Equal direct and bridge-mediated couplings of trajectories with $n = 1$ or 2 are based on few snapshots of low d_{DA} having also high direct coupling between donor and acceptor hence contributing most of mean d_{DA}.

Conformational Analysis. We extracted additional conformational parameters from the trajectories for further analysis on their influence on the coupling. Therefore, we split the oligopeptides into separate groups for every tryptophan and π-system within the oligopeptide chain. For the tryptophans, we take the middle of bond CD2-CE2 as center M of the plane given by the aromatic ring system. For the π-systems, we take atom C as the center of the plane given by the carboxyl group and its neighbored atoms. Between two planes, we define the distance d as the Euclidean distance between their centers, the angle p as the inner angle between the two normal vectors tracking the planarity of the two planes, and finally position angle r as the minimum of the angle between normal vector of the first plane and center of the second plane and vice versa to distinguish planes lying on top of each other from planes being next to each other. Figure 7 depicts d, p, and r between the two tryptophans in Trp-(Pro)2-Trp. We extracted d, p, and r between all adjacent groups as well as between both tryptophans. Here, donor is denoted by D, the acceptor is denoted by A, and the π-systems are counted in ascending order starting at 1 being next to the donor.

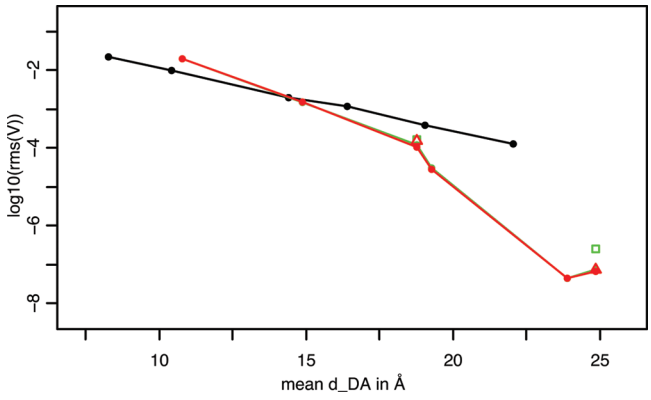

Figure 3. Rms V_{DA} (GMH) values plotted against mean donor−acceptor distance d_{DA} in trajectories of type gas phase (black), solvated-conformation-only (red) and solvated (green). Rms V_{DA} from HF calculations are given for Trp-(Pro)3-Trp and Trp-(Pro)6-Trp for solvated-conformation-only (red triangle) and solvated (green square) trajectories.

We applied PLS-R on all snapshots in gas phase as well as solvated-conformation-only trajectories to analyze the impact of the different conformational parameters on the coupling. Data matrix X is given by derived conformational parameters d, p, and r and Y is V^2_{DA} for each respective trajectory. For normalization, we applied UV scaling on X, assuming a normal distribution, and $\log_{10}$ on Y due to its large range. In general, the PLS-R models for the oligopeptide systems in gas phase have good quality with cumulative Q2 values ranging from 0.34 for Trp-(Pro)6-Trp to 0.53 for Trp-(Pro)2-Trp. The cumulative Q2 of the PLS-R models for oligopeptides in solvated-conformation-only trajectory are lower, ranging from only 0.05 for Trp-(Pro5)-Trp to 0.51 for Trp-(Pro)1-Trp. All models have a maximum of only three principle components (PCs).

The analysis of PLS-R results is based on outcomes of all models from which we show resulting score and loading plots of Trp-(Pro)3-Trp in gas phase (figure 8) as well as Trp-(Pro)3-Trp in solvated-conformation-only (figure 9) as examples. All other PLS-R results can be found in the Supporting Information. Within the score plots, green indicates snapshots with low, yellow medium, and red high coupling values. In all PCs of all models in gas phase, the donor−acceptor distance d_{DA} clearly has the highest loading coefficient, indicated by red bar in Figure 8, meaning that it has the highest influence on the coupling. Results of PLS-R analyses on oligopeptide systems modeled in solvent are not as predictive as those from models in gas phase, indicated by their lower cumulative Q2 values. Overall, they show different behavior from those modeled in gas phase. Within the solvated models, the parameter of highest influence on the coupling V^2_{DA} is not only d_{DA} but, with equally high impact, also $d_{D\text{-}\pi 1}$ and $r_{D\text{-}\pi 1}$ (red bars in Figure 9). Additionally, their loading stays high in PC2 and PC3. Planarity angles p and distances d between the bridging π-systems do not show any influence on the coupling values within the solvent models.

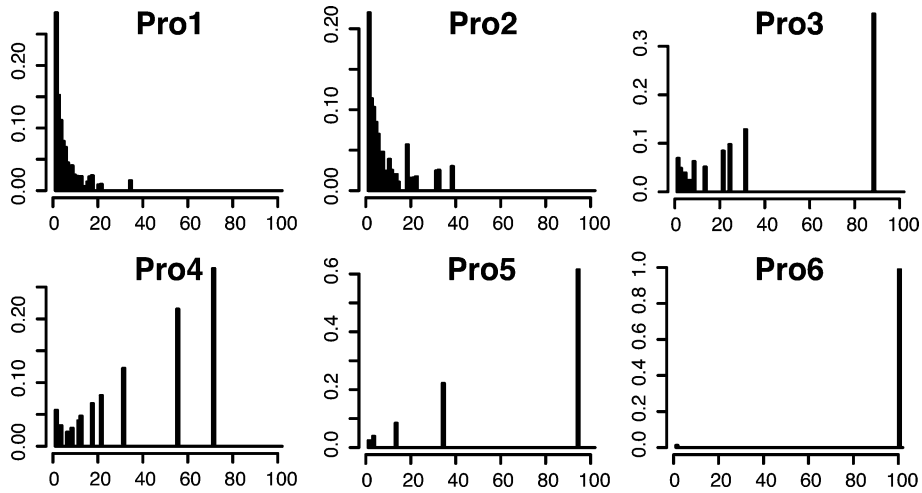

Figure 4. Fraction of mean V^2_{DA} given by data cluster *i* (*y* axes) against z-score of *i* on V^2_{DA} (*x* axes) for trajectories in gas phase. Coupling values higher than 100 z-scores are accumulated into the last cluster.

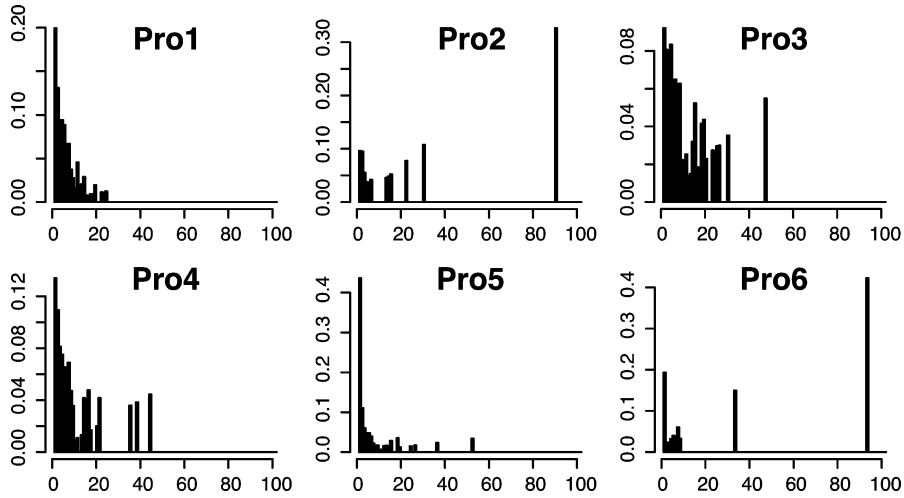

Figure 5. Fraction of mean V^2_{DA} given by data cluster *i* (*y* axes) against z-score of *i* on V^2_{DA} (*x* axes) for solvated-conformation-only trajectories. Coupling values higher than 100 z-scores are accumulated into last cluster.

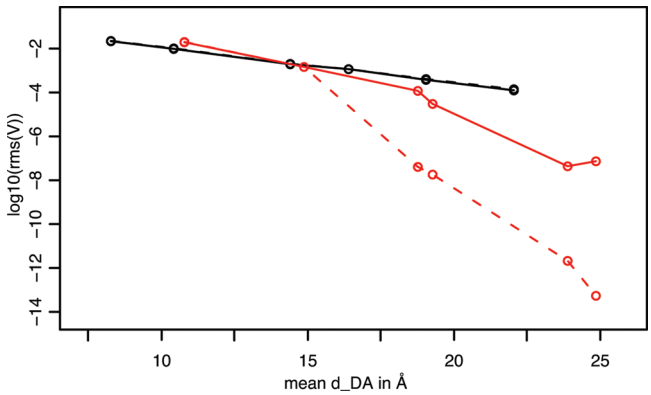

Figure 6. Rms V_{DA} values plotted against mean donor−acceptor distance d_{DA} in gas phase (black) and solvated-conformation-only (red) trajectories. Solid lines indicate bridge mediated couplings and dashed lines only direct couplings between donor and acceptor.

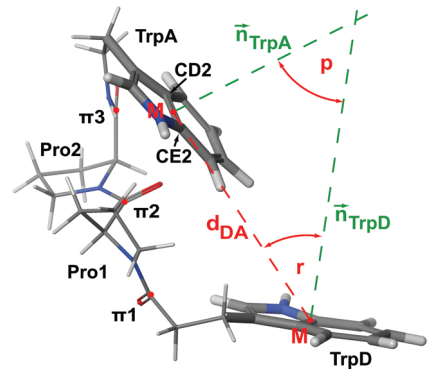

Figure 7. Scheme of conformational parameters distance *d* and angles *p* and *r*, derived from 3D oligopeptide structure. See text for more details.

Translating the influence of the previously detected conformational parameters on the coupling into concrete values derived from the actual snapshots, we calculated the mean values of these parameters extracted from two groups. The first group is snapshots having high coupling, meaning $V^2(x)$ > mean V^2_{DA}, and the second group is the 1000 snapshots lowest in coupling. Figure 10 gives the box plot of significant conformational parameters derived from both groups (high and low coupling) for gas phase as well as solvated-conformation-only trajectories.

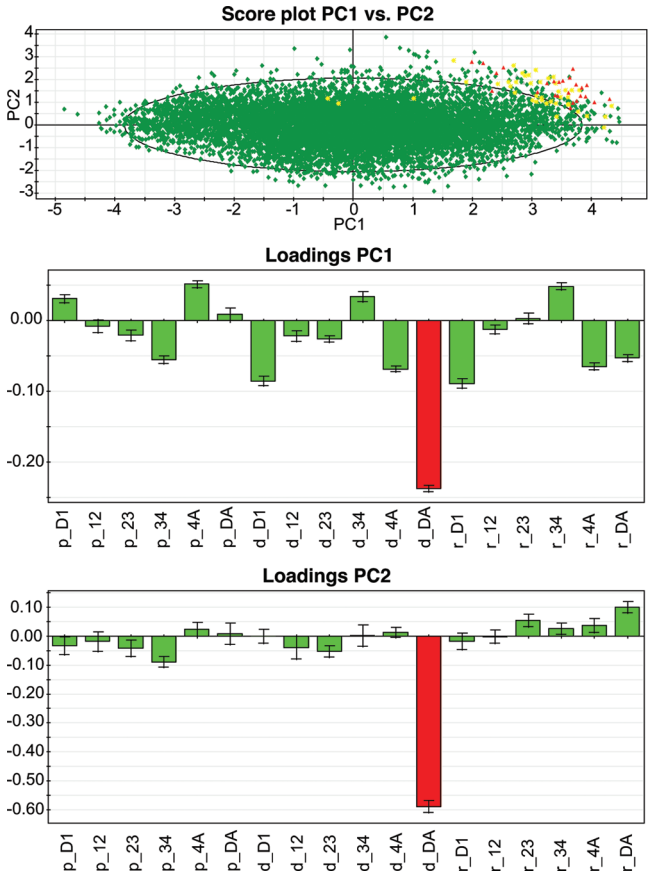

Figure 8. Score and loading plots of PLS-R analysis on Trp-(Pro)3-Trp in gas phase trajectory.

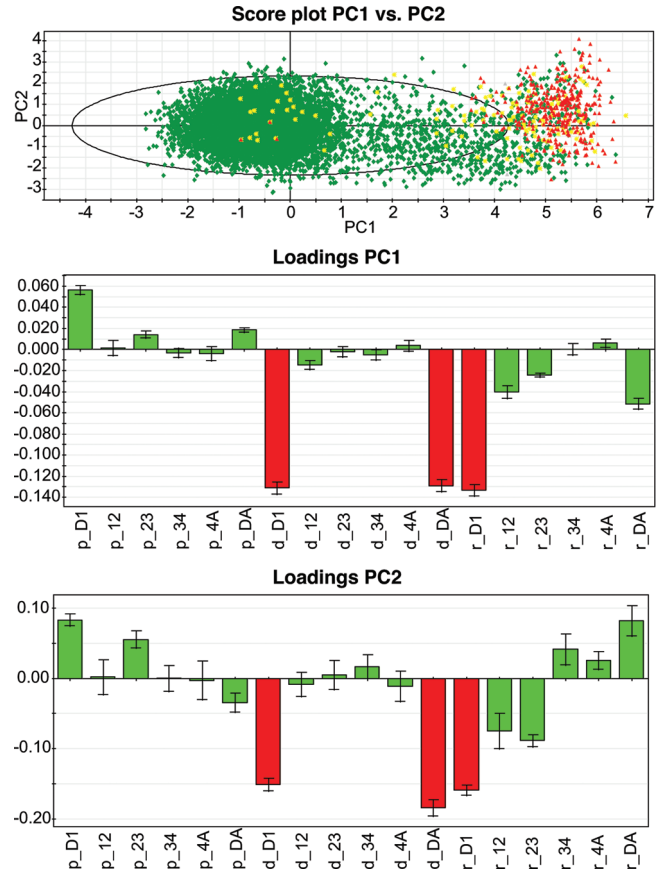

Figure 9. Score and loading plots of PLS-R analysis on Trp-(Pro)3-Trp in solvated-conformation-only trajectory.

In general, there is a clear correlation of shorter distances with high coupling in systems derived from gas-phase simulations as well as in solvated systems. This effect is very strong for the donor−acceptor distance d_{DA} in gas phase. Here, the average values are 5.99 Å for high coupling against 17.48 Å for low coupling. This trend is less clear but still discriminative for the solvated systems where the average d_{DA} for high coupling is 16.43 Å and the average d_{DA} for low coupling is 19.60 Å. The strong loading coefficient of stacking angles $r_{D\text{-}\pi 1}$ in the PLS-R analysis becomes clear when we examine the average values of the two groups. At this point, higher coupling correlates with a smaller angle.

Rate Comparison with Experiments. Isied et al., working on oligoproline peptides with Ruthenium based donors and acceptors, showed that the electron transfer mechanism changes from a predominantly electron superexchange to a predominantly electron hopping when d_{DA} exceeds about 20 Å.[13] Using the parameters from Isied et al. for the reorganization energy, we have computed the ET rates, shown in Figure 11. Analyzing the solvated-conformation-only (red) and solvated (green) plots it seems clear that the linear behavior is broken at $d_{DA} = \sim 20$ Å. At this point, the superexchange ET rate is drastically reduced. These results confirm a possible change in mechanism from superexchange to electron hopping. Future work will address the electron hopping mechanism to confirm this point as the presented study exclusively investigates the superexchange electron transfer mechanism.

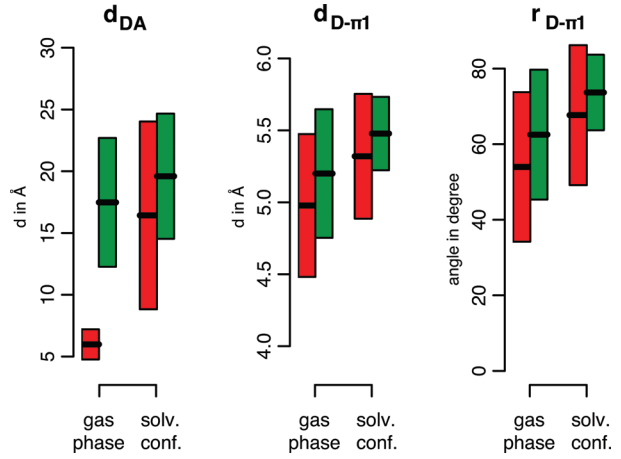

Figure 10. Box plot of conformational parameters extracted from high and low coupling groups of gas-phase and solvated-conformation-only trajectories. Distances *d* measured in Å, angle *r* in degrees. Color code: red = high coupling and green = low coupling.

IV. Conclusions

We have produced a comprehensive study of hole electron transfer in oligoproline peptides of variable length with tryptophan-based donors and acceptors. We have performed extensive molecular dynamics studies and computed the electronic coupling by means of INDO/S semiempirical method and ab initio Hartree−Fock methods (for $n = 3$ and 6). The HF calculations sum up to 40 000 single-point

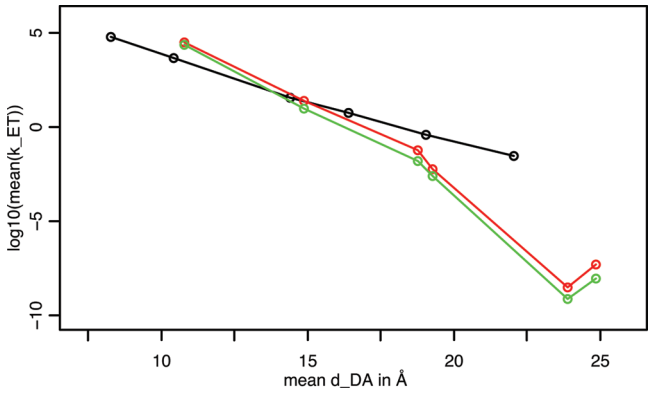

Figure 11. Mean rate constant k_{ET} plotted versus average donor−acceptor distance d_{DA} of oligopeptide in gas-phase (black), solvated-conformation-only (red), and solvated (green) trajectories. Reorganization energy given by ref 13 through $\lambda = \lambda_{in} + \lambda_{out}$, where $\lambda_{in} = 0.085$ eV, $\lambda_{out} = 7.91(1/2a_1 + 1/2a_2 - 1/d_{DA})$ eV and $a_1 = a_2 = 3.3$ Å.

calculations from which we found good agreement between results of semiempirical INDO/S and ab initio HF in the oligopeptides we have investigated. In gas phase, all oligopeptide systems undergo strong conformational changes bringing the two tryptophans in close vicinity, which results in a gated electron transfer mechanism. The dynamics of the oligopeptides in water do not allow for such a close proximity between the donor and acceptor as the number of bridge tryptophans increases, establishing a nongated mechanism where the bridging prolines play a major role in mediating the electronic coupling.

The agreement between the solvated-conformation-only and the solvated results indicate that the water effects are mainly in restricting the conformational space rather than in electronic effects. Whereas the excitation energy E_{12} differs when explicitly adding the water point charges in the one electron Hamiltonian, there is not a large effect of E_{12} on the electronic coupling, as only (diabiatic) orbital overlap accounts. Finally, in agreement with experimental data, our results point to a d_{DA} ~20 Å as a possible point for superexchange to hopping mechanism transition.

Acknowledgment. This work was supported by a grant from the Spanish Ministry of Education and Science to V.G. through the project CTQ2007-62122. Computational resources were provided by the Barcelona Supercomputing Center.

Supporting Information Available: Autocorrelation plot of donor−acceptor distance in 10 ps trajectory of Trp-(Pro)2-Trp in gas phase with 1 ps time steps as well as score and loading plots of all PLS-R analyses on conformational parameters. This material is available free of charge via the Internet at http://pubs.acs.org.

References

(1) Marcus, R. A.; Sutin, N. *Biochim. Biophys. Acta* **1985**, *811*, 265–322.

(2) Newton, M. D. *Chem. Rev.* **1991**, *91*, 767–792.

(3) Beratan, D. N.; Onuchic, J. N.; Winkler, J. R.; Gray, H. B. *Science* **1992**, *258*, 1740–1741.

(4) Gray, H. B.; Winkler, J. R. *Annu. Rev. Biochem.* **1996**, *65*, 537–61.

(5) Balzani, V.; Piotrowiak, P.; Rodgers, M. A. J.; Mattay, J.; Astruc, D.; Gray, H. B.; Fukuzumi, S.; Mallouk, T. E.; Haas, Y.; de Silva, A. P.; Gould, I. R. *Electron Transfer in Chemistry*; Wiley-VCH: Weinheim, Germany, 2001; Vol. I-V.

(6) Ungar, L. W.; Newton, M. D.; Voth, G. A. *J. Phys. Chem. B* **1999**, *103*, 7367–7382.

(7) Isied, S. S.; Ogawa, M. Y.; Wishart, J. F. *Chem. Rev.* **1992**, *92*, 381–394.

(8) Bixon, M.; Giese, B.; Wessely, S.; Langenbacher, T.; Michel-Beyerle, M. E.; Jortner, J. *Proc. Natl. Acad. Sci. U. S. A.* **1999**, *96*, 11713–11716.

(9) Ogawa, M. Y.; Wishart, J. F.; Young, Z.; Miller, J. R.; Isied, S. S. *J. Phys. Chem.* **1993**, *97*, 11456–11463.

(10) Felts, A. K.; Pollard, W. T.; Friesner, R. A. *J. Phys. Chem.* **1995**, *99*, 2929–2940.

(11) Petrov, E. G.; May, V. *J. Phys. Chem. A* **2001**, *105*, 10176–10186.

(12) Berlin, Y. A.; Ratner, M. A. *Radiat. Phys. Chem.* **2005**, *74*, 124–131.

(13) Malak, R. A.; Gao, Z.; Wishart, J. F.; Isied, S. S. *J. Am. Chem. Soc.* **2004**, *126*, 13888–13889.

(14) Shih, C.; Museth, A. K.; Abrahamsson, M.; Blanco-Rodriguez, A. M.; Di Bilio, A. J.; Sudhamsu, J.; Crane, B. R.; Ronayne, K. L.; Towrie, M.; Vlcek, A.; Richards, J. H.; Winkler, J. R.; Gray, H. B. *Science* **2008**, *320*, 1760–1762.

(15) Wittekindt, C.; Schwarz, M.; Friedrich, T.; Koslowski, T. *J. Am. Chem. Soc.* **2009**, *131*, 8134–8140.

(16) Wolfgang, J.; Risser, S. M.; Priyadarshy, S.; Beratan, D. N. *J. Phys. Chem. B* **1997**, *101*, 2986–2991.

(17) Miller, N. E.; Wander, M. C.; Cave, R. J. *J. Phys. Chem. A* **1999**, *103*, 1084–1093.

(18) Castner, E. W.; Kennedy, D.; Cave, R. J. *J. Phys. Chem. A* **2000**, *104*, 2869–2885.

(19) Xie, Q.; Archontis, G.; Skourtis, S. S. *Chem. Phys. Lett.* **1999**, *312*, 237–246.

(20) Skourtis, S. S.; Archontis, G.; Xie, Q. *J. Chem. Phys.* **2001**, *115*, 9444–9462.

(21) Balabin, I. A.; Onuchic, J. *Science* **2000**, *290*, 114–117.

(22) Newton, M. D. *Int. J. Quantum Chem.* **2000**, *77*, 255–263.

(23) Kawatsu, T.; Kakitani, T.; Yamato, T. *J. Phys. Chem. B* **2002**, *106*, 11356–11366.

(24) Balabin, I. A.; Beratan, D. N.; Skourtis, S. S. *Phys. Rev. Lett.* **2008**, *101*, 158102–4.

(25) Skourtis, S. S.; Balabin, I. A.; Kawatsu, T.; Beratan, D. N. *Proc. Natl. Acad. Sci. U. S. A.* **2005**, *102*, 3552–3557.

(26) Zimmt, M. B.; Waldeck, D. H. *J. Phys. Chem. A* **2003**, *107*, 3580–3597.

(27) Troisi, A.; Ratner, M. A.; Zimmt, M. B. *J. Am. Chem. Soc.* **2004**, *126*, 2215–2224.

(28) Lu, S.-Z.; Li, X.-Y.; Liu, W. *Chem. Phys. Lett.* **2005**, *414*, 71–75.

(29) Cave, R. J.; Newton, M. D. *Chem. Phys. Lett.* **1996**, *249*, 15–19.

(30) Cave, R. J.; Newton, M. D. *J. Chem. Phys.* **1997**, *106*, 9213–9226.

(31) Shin, Y.-g. K.; Newton, M. D.; Isied, S. S. *J. Am. Chem. Soc.* **2003**, *125*, 3722–3732.

(32) Liang, C.; Newton, M. D. *J. Phys. Chem.* **1992**, *96*, 2855–2866.

(33) Onuchic, J. N.; Beratan, D. N.; Hopfield, J. J. *J. Phys. Chem.* **1986**, *90*, 3707–3721.

(34) Blancafort, L.; Voityuk, A. A. *J. Phys. Chem. A* **2006**, *110*, 6426–6432.

(35) Zhang, L. Y.; Friesner, R. A. *Proc. Natl. Acad. Sci. U. S. A.* **1998**, *95*, 13603–13605.

(36) Balabin, I. A.; Onuchic, J. N. *J. Phys. Chem.* **1996**, *100*, 11573–11580.

(37) Gehlen, J. N.; Daizadeh, I.; Stuchebrukhov, A. A.; Marcus, R. A. *Inorg. Chim. Acta* **1996**, *243*, 271–282.

(38) Ridley, J.; Zerner, M. *Theor. Chem. Acc.* **1973**, *32*, 111–134.

(39) Voityuk, A. *Chem. Phys. Lett.* **2006**, *427*, 177–180.

(40) Prytkova, T. R.; Kurnikov, I. V.; Beratan, D. N. *J. Phys. Chem. B* **2005**, *109*, 1618–1625.

(41) Lambert, C.; Amthor, S.; Schelter, J. *J. Phys. Chem. A* **2004**, *108*, 6474–6486.

(42) *Maestro, version 8.5*; Schrödinger, LCC: New York, NY, 2008.

(43) *Impact, version 5.0*; Schrödinger, LCC: New York, NY, 2008.

(44) Berendsen, H. J. C.; Postma, J. P. M.; Van Gunsteren, W. F.; Hermans, J. *Intermolecular Forces*, First ed.; Reidel, Dordrecht: 1981; Vol. 331.

(45) Bowers, K. J.; Chow, E.; Xu, H.; Dror, R. O.; Eastwood, M. P.; Gregersen, B. A.; Klepeis, J. L.; Kolossvary, I.; Moraes, M. A.; Sacerdoti, F. D.; Salmon, J. K.; Shan, Y.; Shaw, D. E. In *Proceedings of the 2006 ACM/IEEE Conference on Supercomputing*; ACM: Tampa, FL, 2006, 84.

(46) Jorgensen, W. L.; Tirado-Rives, J. *Proc. Natl. Acad. Sci. U. S. A.* **2005**, *102*, 6665–6670.

(47) Voityuk, A. A.; Rosch, N. *J. Chem. Phys.* **2002**, *117*, 5607–5616.

(48) Jordan, K. D.; Paddon-Row, M. N. *J. Phys. Chem.* **1992**, *96*, 1188–1196.

(49) *Jaguar, version 7.5*; Schrödinger, LCC: New York, NY, 2008.

(50) *R: A Language and Environment for Statistical Computing*, R Foundation for Statistical Computing: Vienna, Austria, 2007.

(51) Wold, S.; Sjöström, M.; Eriksson, L. *Chemom. Intell. Lab. Syst.* **2001**, *58*, 109–130.

(52) Hoffman, B. M.; Ratner, M. A. *J. Am. Chem. Soc.* **1987**, *109*, 6237–6243.

CT900377J